

# Impact of wind generation uncertainty on power system small disturbance voltage stability: A PCM-based approach

Ce Zheng\*, Mladen Kezunovic

Department of Electrical and Computer Engineering, Texas A&M University, College Station, TX 77843-3128, USA

## ARTICLE INFO

### Article history:

Received 7 June 2011

Received in revised form 1 September 2011

Accepted 6 October 2011

Available online 28 October 2011

### Keywords:

Small disturbance

PCM

Uncertainty

Wind generation

Voltage stability

Eigenvalue

Probability density function

## ABSTRACT

The connection of wind generators with electric power system influences the system stability and nodal voltages. This paper performs uncertainty analysis to investigate the impact of wind generation variation on the small disturbance voltage stability. The probabilistic collocation method (PCM) is presented as a computationally efficient method to conduct the uncertainty analysis. It has been implemented in a simple system to demonstrate its applicability in analyzing wind generation uncertainty. More case studies on a larger system are conducted to obtain a deeper understanding of how the system voltage stability is affected by the integration of DFIG-based wind farms. As compared with the traditional Monte Carlo simulation method, the collocation method could provide a quite accurate approximation for the eigenvalue probabilistic distribution with fewer simulation runs.

© 2011 Elsevier B.V. All rights reserved.

## 1. Introduction

As wind generation continues to expand in size and penetration level, a deeper understanding of its dynamic behavior and impact on system stability becomes necessary. Since the wind farm production is primarily determined by wind speed and thus fluctuating constantly, one of the most important studies is to investigate the dynamic phenomena induced by the variation of wind generation.

Historically power system stability has been associated with the generator rotor angle dynamics. Stimulated by several major voltage collapses, the framework of power system voltage stability as defined in [1] was originated around 1980s [2,3] and had been extensively studied in 1990s [4,5]. Voltage stability can be further classified into small disturbance and large disturbance categories. The small disturbance voltage stability refers to the system's ability to maintain steady voltage levels following small disturbances experienced through continuous changes in load [6–8]. From this view the small disturbance voltage stability is predominantly load stability. With the recent rapid growth of wind generation, operational uncertainty will extend from demand side

variability to a significant portion of the supply side variability as well, which will impact system dynamic performance and cause voltage deviations. As a result, it is imperative to take into account the stochastic nature of wind farm output in voltage stability study.

From the end of the last century, the wind generators based on fixed-speed wind turbines have been included in stability studies [9–11]. Later, the grid stability enhancement of the new variable-speed wind generators, especially the Doubly-Fed Induction Generators (DFIG), has been reported in several publications [12–14]. Recently, research efforts to study how further large scale integration of variable-speed wind generators will influence the power system stability and electricity market have been proposed [15].

While such studies are important in their own right, the important issue of how the system small disturbance voltage stability may be influenced by the constantly changing wind generation has not been fully explored yet.

A review of literature reveals that several studies have been reported in the related area. Refs. [16,17] conducted modal and eigenvalue sensitivity analysis on grid-connected DFIGs. The work reported in [18] explored the relationship between uncertain wind generation and system probabilistic small-signal stability analysis via Monte Carlo simulation method.

As very few tools are available to analyze the parameter uncertainties in time-domain simulations, Tatang et al. developed the

\* Corresponding author. Tel.: +1 979 595 8859; fax: +1 979 845 9887.

E-mail addresses: [zhengce@neo.tamu.edu](mailto:zhengce@neo.tamu.edu) (C. Zheng), [kezunov@ece.tamu.edu](mailto:kezunov@ece.tamu.edu) (M. Kezunovic).

probabilistic collocation method (PCM) to mathematically describe the system response in terms of uncertain parameters [19]. This method has been successfully applied to time-domain simulation studies in the area of global climate change [20]. Later in [21], Hockenberry et al. have introduced the probabilistic collocation method in power system dynamic analysis and discussed its applicability in load uncertainty analysis. More studies have been reported to evaluate the advantage of PCM over other uncertainty analysis techniques in the time-domain analysis of power system load parameter uncertainties [22].

Normally the uncertainty analysis is performed under one of the following situations:

- (1) The relationship between the uncertain parameter and the output of interest is known analytically;
- (2) The above relationship is unknown. A model of the “black box” needs to be approximated first.

The PCM is designed to address the second situation. This approach allows the use of nonlinear models and evaluation of complicated output functions. It is particularly appealing because it requires a much smaller number of simulations to reach an accurate approximation which may take hours or days for the traditional techniques.

This paper studies how wind generation variation will impact voltage stability under the new energy transfer scenario where traditional generators are supplanted by variable-speed wind generators. Since the relationship between uncertain wind generation and system small disturbance voltage stability is not analytically clear, the PCM is introduced to address the problem. It begins with the mathematical definitions of the collocation method. Then, the wind-connected power system dynamic modeling and small disturbance analysis procedures are provided in Section 3. Sections 4 and 5 constitute the key aspects of the paper. First, a simple system is established to explore the applicability of implementing PCM in the wind generation uncertainty analysis. Next, a more complicated 23-bus power system is presented. Deeper understanding is obtained by monitoring the eigenvalue movement and voltage instability induced by the variation of wind farm output. The computation efficiency of PCM has been demonstrated by comparing it with traditional simulation based approaches.

## 2. Probabilistic collocation method

The basic idea of PCM is to approximate the relationship between uncertain parameters of the system and the outputs of interest through polynomial models. Based on the probability density function of the uncertain parameters, the concepts of orthogonal polynomials and Gaussian Quadrature Integration are incorporated to solve for polynomial approximation functions. Once the polynomials are obtained, collocation methods are generated to solve for the model coefficients. One major advantage of PCM is that only a handful of simulations are needed to determine the approximation model.

### 2.1. PCM with multiple inputs

To be general, let  $x_1, x_2, \dots, x_n$  be the uncertain parameters. Suppose a system is represented by a complex, high-ordered, or even “black-box” model. Its response in terms of the uncertain parameters is expressed as:

$$U = P(x_1, x_2, \dots, x_n) \quad (1)$$

where  $U$  is the output of interest (system response). The objective of PCM is to find the following approximation of  $U$ :

$$\begin{aligned} \hat{U} = & C_0 + \sum_{i=1}^n [C_{i1}p_{i1}(x_i) + C_{i2}p_{i2}(x_i) + \dots + C_{im}p_{im}(x_i)] \\ & + \sum_{i=1}^n \sum_{\substack{j=1 \\ j \neq i}}^n [C_k p_{i1}(x_i) p_{j1}(x_j)] \end{aligned} \quad (2)$$

where  $\hat{U}$  is an approximation of  $U$ ,  $m$  is the order of this polynomial model,  $C_0, C_{i1}, \dots, C_{im}, C_k$  are model coefficients, and  $p_{i1}(x_i), p_{i2}(x_i), \dots, p_{im}(x_i)$  are polynomial functions in terms of each uncertain parameter  $x_i$ .

### 2.2. Solving for polynomials

What we need then is to find the set of polynomials and coefficients listed in (2). The polynomials could be derived by deploying the concept of orthogonal polynomials [23]. The definition of orthogonal polynomials is:

$$\int_x P(x)H_i(x)H_j(x)dx = \begin{cases} 1, & \text{if } i=j \\ 0, & \text{if } i \neq j \end{cases} \quad (3)$$

where  $P(x)$  is user-defined weighting function of  $x$ ,  $H_i(x)$  and  $H_j(x)$  are orthogonal polynomials of  $x$  with the order of  $i$  and  $j$  ( $i, j = 0, 1, \dots$ ). Eq. (3) suggests that the inner product of any two orthogonal polynomials of different order is always zero.

Assume the probability density function of the  $i$ th uncertain parameter is  $f(x_i)$ . By substituting the weight function  $P(x)$  with  $f(x_i)$ , and using the following definition:

$$H_{-1}(x) = 0, \quad H_0(x) = 1 \quad (4)$$

the remaining higher-order orthogonal polynomials can be derived one by one. Fitting the derived orthogonal polynomials to  $p_{i1}(x_i), p_{i2}(x_i), \dots, p_{im}(x_i)$  of (2), only the coefficients are left to be solved.

### 2.3. Solving for coefficients

As long as the polynomial functions in (2) are known, the model coefficients can be calculated by feeding different inputs into the system and recording corresponding system response. Suppose the system has  $n$  uncertain parameters, and we are using a PCM model with the order of  $m$ , the sets of inputs that are needed will be:

$$1 + n \times m + \binom{n}{2} \quad (5)$$

Take the linear PCM model with single uncertain parameter  $x$  as an example, Eq. (2) could be rewritten as:

$$\hat{U} = C_0 + C_1 p_1(x) \quad (6)$$

What we need next is to feed the real system with two different values of parameter  $x$ , and substitute  $\hat{U}$  with the real system response  $U$  of each run. Thus the coefficients  $C_0$  and  $C_1$  in (6) could be solved.

In the above linear model example, the two different input values are also called collocation points. It should be noted that the selection of collocation points has significant impact on the accuracy of model approximation. In order to find a good approximation for the PCM model with smallest number of model runs, the Gaussian Quadrature Integration [23] approach is deployed: while selecting the collocation points, the points for the model runs from the roots of the next higher order orthogonal polynomial will

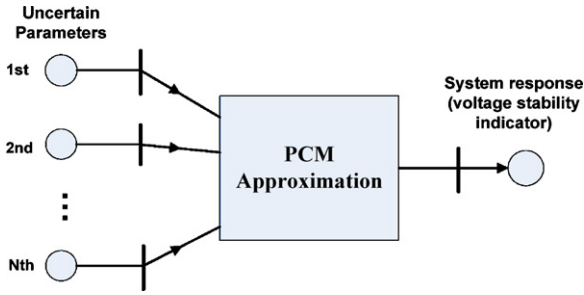


Fig. 1. PCM approximation used for voltage stability analysis.

be selected for each uncertain parameter. This approach enables the collocation points spanning the high probability regions of their distribution and capturing as much of the behavior of system response as possible.

The whole idea of applying PCM in power system uncertainty analysis is demonstrated in Fig. 1. Selected set of uncertain parameters is fed into the full dynamic model of a power system and corresponding output of interest is recorded. The relationship between uncertain parameters and system response is then approximated through PCM once sufficient tests are conducted. In this work, our output of interest is the ‘voltage stability indicator’, which essentially monitors the stability of system voltage following small disturbances experienced through continuous changes in wind farm production. An eigenvalue-based indicator is defined in the follow-up sections.

### 3. Small disturbance voltage stability

Voltage stability has long been evaluated by both static and dynamic approaches while it essentially has dynamic nature. This paper investigates the small disturbance (SD) voltage stability problem caused by fluctuation in wind generation from the viewpoint of its dynamical mechanism.

In a power system, on-load tap changing transformers and thermal units in charge of load frequency control are working slowly in a time frame of minutes, while generators, automatic voltage regulators, governors and induction motor loads respond much faster. Therefore, the power system can be approximated by two simplified systems: slow and fast response subsystems [4,5]. Their dynamic behavior can be described by a set of differential equations:

$$\dot{x}_S = f_S(x_S, V, u) \quad (7)$$

$$\dot{x}_F = f_F(x_S, x_F, V, y, z, u, \text{load}) \quad (8)$$

where  $x_S$  and  $x_F$  represents system slow and fast response state variables respectively,  $u$  represents the controllable variables,  $\text{load}$  represents uncontrollable variable vector which governs load consumption,  $V$  is the bus voltage vector,  $y$  is the node specification vector in load flow equation, and  $z$  is the dependent variable vector. Eqs. (7) and (8) stand for all the dynamic characteristics existing in the whole system. The static relationships in loads and generating units, etc., are usually described by a set of algebraic equations:

$$0 = g_F(x_S, x_F, V, y, z, u, \text{load}) \quad (9)$$

$$y = g_N(x_S, x_F, V, u) \quad (10)$$

A common approach to evaluate the voltage stability of a fast subsystem is through linearization of its differential equations and eigenvalue analysis. Slow variables  $x_S$  are treated as constant. Fixing

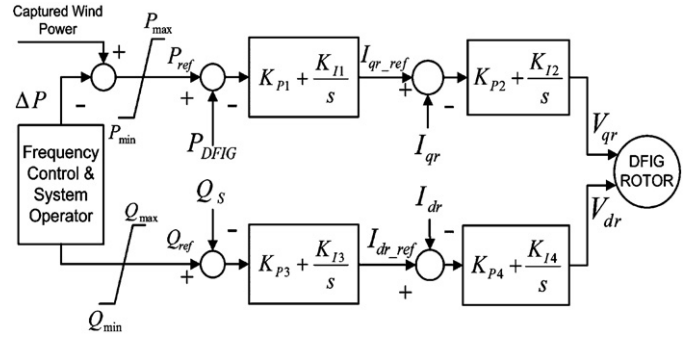


Fig. 2. DFIG frequency (top) and reactive power (bottom) controllers.

$u$  and  $\text{load}$ , Eqs. (8)–(10) are linearized around system equilibrium point by eliminating both  $y$  and  $z$ :

$$\begin{bmatrix} \Delta \dot{x}_F \\ 0 \end{bmatrix} = \begin{bmatrix} H_F & H_V \\ Y_F & J_N - Y_V \end{bmatrix} \begin{bmatrix} \Delta x_F \\ \Delta V \end{bmatrix} \quad (11)$$

The state-space matrices  $H_F$ ,  $H_V$ ,  $Y_F$ ,  $J_N$  and  $Y_V$  are defined in [4]. By eliminating  $\Delta V$ , the linearized fast response subsystem could be presented as:

$$\Delta \dot{x}_F = [H_F - H_V(J_N - Y_V)^{-1}Y_F]\Delta x_F = A_{FF}\Delta x_F \quad (12)$$

The matrix  $A_{FF}$  is formulated from system differential algebraic equations (DAE), which are detailed by dynamic modeling of each network component.

#### 3.1. DAE of doubly fed induction generator

Dynamic modeling of the DFIG-based wind generator is realized by modeling of its several components: wind turbine, shaft, generator, converter, and control system [9]. While there is a general acceptance of models for wind turbine, drive train (shaft), and induction generator, a variety of modeling schemes for the frequency and VAR controllers are being used nowadays. The DFIG frequency and VAR controllers adopted in this work are represented in Fig. 2 [9]:

The differential equations to describe the dynamic behavior of a DFIG are derived and listed in (13) and (14):

$$\begin{cases} \dot{E}'_q = -\frac{1}{T'_0} [E'_q + (X_s - X'_s)I_{ds}] + \left[ \omega_s \frac{X'_m}{X'_r} V_{dr} - (\omega_s - \omega_r)E'_d \right] \\ \dot{E}'_d = -\frac{1}{T'_0} [E'_d + (X_s - X'_s)I_{qs}] + \left[ -\omega_s \frac{X'_m}{X'_r} V_{qr} + (\omega_s - \omega_r)E'_q \right] \\ \dot{\omega}_r = \frac{\omega_s}{2H} (T_m - E'_d I_{ds} - E'_q I_{qs}) \end{cases} \quad (13)$$

$$\begin{cases} \dot{m}_1 = K_{I3}[Q_{ref} - (Q_r + Q_s)] \\ \dot{m}_2 = K_{I4}\{K_{P3}[Q_{ref} - (Q_r + Q_s)] + m_1 - I_{dr}\} \\ \dot{m}_3 = K_{I1}[P_{ref} - (P_r + P_s)] \\ \dot{m}_4 = K_{I2}\{K_{P1}[P_{ref} - (P_r + P_s)] + m_3 - I_{qr}\} \end{cases} \quad (14)$$

In (14),  $m_1$ – $m_4$  are state variables associated with the reactive power and frequency PI controllers. The definition of the state variables and constants included in (13) and (14) could be found in [9,17]. The algebraic equations of DFIG are derived in Appendix A.

#### 3.2. DAE of electric grid

Using the dynamic modeling process described in [4,6], the DAEs for the remaining components of the electric network, including synchronous machines, other types of generators, induction

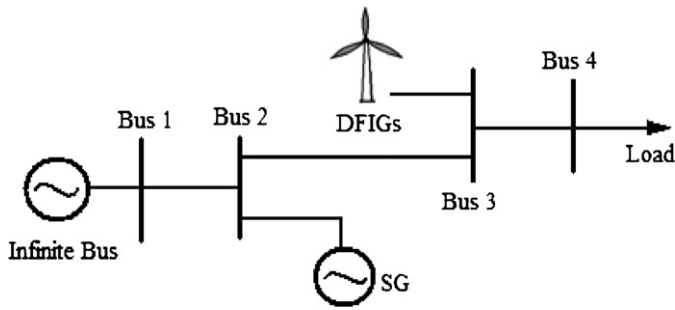


Fig. 3. Four-bus test system with a local wind farm at Bus 3.

motors, FACTS devices, load and tap-changing transformers are formulated. By combining the network DAE with the set of DFIG DAE, the overall set of state variables  $x_F$ , as well as matrices  $H_F$ ,  $H_V$ ,  $Y_F$ ,  $J_N$ ,  $Y_V$  and  $A_{FF}$  in (11) and (12) can be determined.

### 3.3. Small disturbance voltage stability evaluation

The SD voltage stability analysis essentially monitors the eigenvalue trajectory of the matrix  $A_{FF}$  in (12). For a given wind generation level, using the DAEs formulated in the previous steps, a system state matrix  $A_{FF}$  can be uniquely decided. Calculating the eigenvalues of  $A_{FF}$  at each operating point, the system SD voltage stability can be evaluated by checking if all the eigenvalues are located in the left hand half of the complex plane. The fast response subsystem is losing voltage stability when one of the real parts of the eigenvalues of  $A_{FF}$  vanishes. The critical voltage stability point is identified when one of the eigenvalues reaches imaginary axis.

Note that although the above treatment is generally accepted and widely used, there is still a lack of mathematical validation of the treatment. However, rigorous numerical simulation studies have demonstrated that the singularity or sign change of determinant of system Jacobian matrix always indicates the loss of voltage stability [3–5]. Hence the above eigenvalue monitoring approach seems valid when studying the voltage problems in a power system. To verify the above treatment, a linear voltage stability indicator detailed in [24,25] will be used to compare the results of the proposed eigenvalue-based indicator.

## 4. Implementation of PCM in a simple system

In this section, the collocation method will be applied in the uncertainty analysis of a simple four-bus system to demonstrate its validity. The system one-line diagram is illustrated in Fig. 3, in which the DFIG-based wind farm is connected at Bus 3.

### 4.1. Parameter specification

It is necessary to determine the uncertain parameters and corresponding output of interest in Fig. 1 before conducting uncertainty analysis. In the test system, the wind speed  $v_{wind}$  is selected as the single uncertain parameter. As discussed earlier, the real part of the critical eigenvalues  $Eig_{real}$  of matrix  $A_{FF}$  is able to indicate the SD voltage stability. Hence it is selected as the output of interest. The relationship between  $v_{wind}$  and  $Eig_{real}$  is analytically clear. The time-varying wind speed will constantly change the nodal injection of the wind farm at its point of common coupling (PCC), which has significant impact on the system load flow and oscillation modes. Therefore the variation of wind speed will influence the distribution of critical eigenvalues on the complex plane.

The DFIG dynamic model presented in the previous section is adopted, with the rated power, cut-in, cut-out and rated wind

Table 1  
1st to 6th order orthogonal polynomials for standard Gaussian distribution  $\delta$ .

Order	Orthogonal polynomials	Roots
1st	$\delta$	{0}
2nd	$\delta^2 - 1$	{-1, 1}
3rd	$\delta^3 - 3\delta$	{-1.7321, 0, 1.7321}
4th	$\delta^4 - 6\delta^2 + 3$	{-2.3344, -0.7420, 0.7420, 2.3344}
5th	$\delta^5 - 10\delta^3 + 15\delta$	{-2.8570, -1.3556, 0, 1.3556, 2.8570}
6th	$\delta^6 - 15\delta^4 + 45\delta^2 - 15$	{-3.9694, -3.4839, -j3.5908, j3.5908, 3.4839, 3.9694}

speeds specified as 3.6 MW, 4 m/s, 20.9 m/s and 12.9 m/s respectively.

Also, the probability density function (PDF) of the uncertain parameter needs to be specified beforehand. In our research, the wind speed with a Gaussian distribution is assumed first. This is only for the purpose of illustrating the calculation process of PCM, although it may not be realistic. A more widely used Weibull distribution will be adopted and examined in the next section. With the combination of energy storage, the wind farm injection instead of the wind speed will be taken as the input parameter for PCM. Under this situation, PDFs other than the Weibull distribution, such as the normal distribution, need to be considered.

The PDF of a Gaussian distribution is:

$$f(v_{wind}) = \begin{cases} \frac{1}{\sqrt{2\pi\sigma^2}} e^{-((v_{wind}-\mu)^2/2\sigma^2)}, & v_{wind} \geq 0 \\ 0, & v_{wind} < 0 \end{cases} \quad (15)$$

When  $v_{wind} \geq 0$ , a mean of  $\mu = 9$  and a standard deviation of  $\sigma = 2$  are assumed.

### 4.2. Polynomial approximation

What we need then is to approximate the relationship between the uncertain parameter  $v_{wind}$  and system response  $Eig_{real}$  based on the PDF of wind speed. A “variable transformation” is applied in PCM: the random variable  $X$  with any kind of Gaussian distribution will be represented by the following transformation:

$$X = \mu + \sigma[p_1(\delta)] \quad (16)$$

where  $p_1(\delta)$  is the first order orthogonal polynomial of the standard normal distribution  $\delta$ , which has a mean value of  $\mu_\delta = 0$  and a standard deviation of  $\sigma_\delta = 1$ . The advantage of this transformation lies in the convenience of using same orthogonal polynomials to stand for any Gaussian distribution [19,20].

The Hermite Polynomials designed for standard normal distribution are deployed to derive orthogonal polynomials. The first to sixth order polynomial expressions and their respective roots are listed in Table 1. The roots of the involved polynomials are listed for the Gaussian Quadrature Integration method to generate collocation points.

Eq. (2) will be solved using the generated collocation points and corresponding system responses. Note that for the case of a single uncertain parameter and  $m$ th order PCM model, the number of required collocation points, according to (5), is  $m + 1$ .

The algorithm steps and pseudocode to obtain the polynomial model between the uncertain parameter  $v_{wind}$  and system response  $Eig_{real}$  are summarized in Table 2 (description of how to calculate SSR for model error evaluation will be introduced later).

### 4.3. Discussion

Although the nodal injection power of a wind farm is primarily determined by the on-site wind speed, several other factors may influence its value in normal practice. For example, wind generation may vary along with the real time electricity prices. The setting of

**Table 2**  
Algorithm steps: polynomial approximation between  $v_{wind}$  and  $Eig_{real}$ .

1.	Choose threshold $\varepsilon$
2.	Specify the PDF of $v_{wind}$ : $f(v_{wind})$ Perform variable transformation (e.g. Eq. (16)) if needed Substitute into Eqs. (3) and (4):
3.	$\int_{-\infty}^{\infty} f(v_{wind})H_1(x)(1)dx = 0, \int_{-\infty}^{\infty} f(v_{wind})H_2(x)H_1(x)dx = 0,$
4.	Solve for the orthogonal polynomials: $H_1(x), H_2(x), \dots, H_N(x)$
5.	Repeat: for $k=1 \rightarrow N$ do find the roots of $H_{k+1}(x)$ : $R_1, R_2, \dots, R_{k+1}$ run model on collocation points $R_1, R_2, \dots, R_{k+1}$ substitute $\hat{U}$ in Eq. (2) with the model output $Eig_{real}$ solve the coefficients of Eq. (2): $C_0, C_1, \dots, C_{k+1}$ end for SSR $\leq \varepsilon$ (SSR calculated from Eq. (19))
6.	Use approximation for uncertainty analysis

wind turbine controllers may be switched between terminal voltage control mode and power factor control mode. System operators may request the wind farm to adjust its output level according to the frequency control requirements. In addition, the system voltage stability is dependent on a number of stochastic system parameters such as load fluctuations and equipment outages. Under these situations, the problem is more complicated and system response is harder to predict. However, it is still possible for PCM to approximate the relationship by taking into account multiple uncertain parameters. The polynomial model will be expanded according to Eqs. (1) and (2) described in Section 2.1.

Suppose we are considering two uncertain parameters, that is, load total active power demand  $P_L$  and wind power injection  $P_{wind}$ . The new PCM expansion will be:

$$\hat{U} = C_0 + C_1 H_1(P_L) + C_2 H_1(P_{wind}) + C_3 H_2(P_L) + C_4 H_2(P_{wind}) + \dots + C_n H_1(P_L) H_1(P_{wind}) \quad (17)$$

As shown in (17), for a model which is second-order or higher, a cross-product term is added to the end of the expansion for higher approximation accuracy. In the above example, the collocation points (roots) will be derived for  $P_L$  and  $P_{wind}$  separately. Different pairs of roots will be formed using different combinations. The ranking of the combinations is arranged according to the probability of the involved roots. The first pair will always be the highest probability root for each parameter, which is the so-called ‘‘anchor point’’. Also, one more input pair is needed corresponding to the cross-product term. For this we use the second-highest probability root of  $P_L$  and  $P_{wind}$  respectively.

Nevertheless, the wind speed is chosen as the single uncertain parameter in this research for the purpose of not adding complexity to the problem. The merit of doing this is that the relationship between  $v_{wind}$  and  $Eig_{real}$  could be clearly identified. Further, the

power factor control for all DFIGs in a wind farm is assumed, which complies with the grid code of most power systems in the United States.

The incorporation of energy storage units help address uncertainty in wind generation and modern forecasting technique is sufficiently mature that wind speed could be predicted with acceptable accuracy. This helps to relieve the stochastic nature of wind farm output, yet it does not contradict with the proposed method:

- The supply side variability introduced by renewable generations shall not be overlooked. Energy storage system compensates uncertainty; however it does not eliminate the variation. Operational constraints such as limited capacity of storage units limit the maximum generation commitment that can be met reliably by a wind farm;
- Knowing exactly how much power will be generated can actually help to take advantage of the PCM technique, that is, the PDF of wind farm output will be less dependent on the on-site historical data but can be extracted from the forecasted values;
- The proposed method is able to establish a computationally less expensive link between the wind farm output and system SD voltage stability. As engineers try to capture more detail and complexity of the power system dynamic processes, the models become more complex to run. This simplification makes the proposed method particularly appealing.

We will next discuss the difference of the PCM model when wind speed falls in different zones divided by the DFIG cut-in speed  $v_{in}$ , cut-out speed  $v_{out}$  and rated wind speed  $v_{rated}$ . The mechanical power extracted from the wind turbine is given as:

$$P_m = \begin{cases} 0 & v_{wind} < v_{in}; v_{out} \leq v_{wind} \\ g(v_{wind}) & v_{in} \leq v_{wind} < v_{rated} \\ P_{rated} & v_{rated} \leq v_{wind} < v_{out} \end{cases} \quad (18)$$

where  $g(v_{wind}) = 1/2 \rho A_{wt} C_p(\lambda, \theta) v_{wind}^3$ , in which  $\rho$  is the air density,  $A_{wt}$  is the wind turbine swept area, and  $C_p$  is function of tip speed ratio  $\lambda$  and pitch angle  $\theta$  [4]. An observation of (18) is that the system response should be discussed differently as the way the mechanical power is divided. This means although the PDF of wind speed is continuous, the system may respond in a discrete manner. So the relationship between  $v_{wind}$  and  $Eig_{real}$  should be treated carefully in PCM. The system response  $Eig_{real}$  should be modeled as:

$$Eig_{real} = \begin{cases} P_1(v_{wind}) & S1 : v_{wind} < v_{in} \& v_{out} < v_{wind} \\ P_2(v_{wind}) & S2 : v_{in} < v_{wind} < v_{rated} \\ P_3(v_{wind}) & S3 : v_{rated} < v_{wind} < v_{out} \end{cases} \quad (19)$$

**Table 3**  
Collocation points, critical eigenvalues, and calculated coefficients for 1st to 4th order model under the second situation S2.

Order	Collocation points	Corresponding wind speed (m/s)	Real part of critical eigenvalues $Re\{\lambda(A_{FF})\}$	Calculated coefficients
1st	-1	7	0.08200	$C_0 = -0.0697$
	1	11	-0.22130	$C_1 = -0.1517$
	-1.7321	5.5358	0.39060	$C_0 = -0.0521$
2nd	0	9	-0.10702	$C_1 = -0.1920$
	1.7321	12.4642	-0.27450	$C_2 = 0.0551$
	-2.3344	4.3312	0.60692	$C_0 = -0.0694$
3rd	-0.7420	7.5160	0.01757	$C_1 = -0.1715$
	0.7420	10.4840	-0.20061	$C_2 = 0.0492$
	2.3344	13.6688	-0.30839	$C_3 = -0.0100$
4th	-2.8570	3.2860	0.82942	$C_0 = -0.0544$
	-1.3556	6.2888	0.18819	$C_1 = -0.1835$
	0	9	-0.10702	$C_2 = 0.0473$
	1.3556	11.7112	-0.24875	$C_3 = -0.0040$
	2.8570	14.7140	-0.33729	$C_4 = -0.0018$

**Table 4**  
Error evaluation for 1st to 3rd order PCM approximation under the situation of S2.

Order	Expected $\hat{Y}$	SSR
1st	-0.0697	0.0602
2nd	-0.0521	0.0274
3rd	-0.0694	0.0075

where  $P_1$ ,  $P_2$  and  $P_3$  are PCM models under the situations of S1, S2 and S3 respectively.

The formulation for first to third order models under the situation of S2 is given in Table 3. The dominant state variables of the critical eigenvalues are speed deviation  $\omega_{SG}$  and angle deviation  $\theta_{SG}$  of the synchronous generator at Bus 2. It can be observed that in 3rd and 4th order models, sometimes we need to obtain  $Eig_{real}$  even when  $v_{wind}$  is out of the interval of S2. In such cases, we still assume that the wind generation keeps increasing/decreasing even if the wind speed goes beyond the rated speed or drop below the cut-out speed. This makes sure the model approximation could accurately reflect the system dynamic behavior within S2.

#### 4.4. Error evaluation

By feeding the generated collocation points into the test system, the corresponding critical eigenvalues are obtained. The coefficients of the PCM model could then be solved by substituting into (2). The calculated coefficients are also listed in Table 3.

Last but not least, the approximation error should be evaluated to guarantee the model accuracy. In this work, the Sum-Square-Root (SSR) error is calculated:

$$SSR = \sqrt{\frac{\sum_{i=1}^j [(\hat{Y}_i - Y_i)^2 \times f(\delta_i)]}{f(\hat{\delta}) \times j}} \quad (20)$$

where  $Y$  is the real system response and  $\hat{Y}$  is the PCM approximation,  $j$  is the number of collocation points generated for error evaluation,  $f(\delta_i)$  is the PDF at the value of  $\delta_i$ , and  $\hat{\delta}$  is the collocation point with highest probability.

To check the error, the collocation points derived from the next higher order orthogonal polynomials are used to run the model several more times. The error evaluation results for 1st to 3rd order models are shown in Table 4.

A larger SSR indicates a larger deviation of PCM model approximation from real system behavior and vice versa. In this case an error criterion of  $1 \times 10^{-2}$  is assumed. From Table 4 it can be concluded that the linear and quadratic models have poor approximations and should not be deployed. The third order model, with an acceptably small SSR, is able to represent the relationship between  $v_{wind}$  and  $Eig_{real}$  more accurately.

#### 4.5. Comparison with linear voltage collapse indicator

The above obtained PCM model will be compared with a linear Voltage Collapse Indicator (VCI) first reported in [24,25]. The test system has been simplified to a two-bus system: the Thevenin equivalent is derived for the network to the left of Bus 3; the wind farm, treated as negative load, is combined with the load at Bus 4. Preliminary results are shown in Fig. 4. Note that while the abscissa for PCM model is wind speed, we use the wind farm MW injection as input for VCI.

It can be concluded from Fig. 4 that with the decrease of wind speed (hence the wind farm injection), there is an agreement of the two indicators to their voltage instability point (0 for the eigenvalue indicator and 1 for VCI). We can also observe that compared with the linear VCI, the third-order PCM model exhibits a non-linear characteristic.

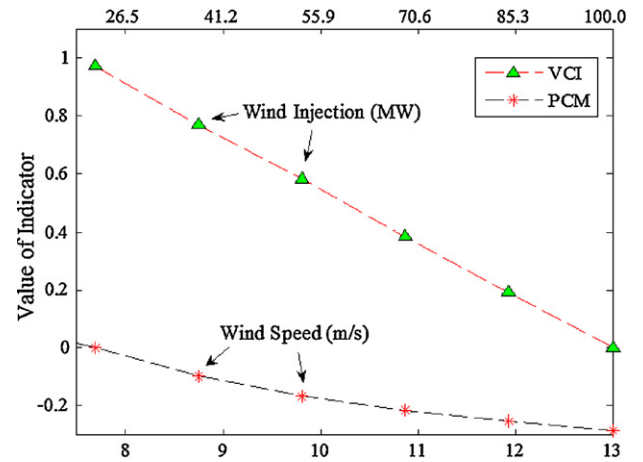


Fig. 4. Comparison of the linear VCI and the PCM model.

**Table 5**  
PCM approximation for situations S1 and S3.

Situation	Critical eigenvalues	PCM model
S1 (cut out)	$1.1376 \pm j5.0616$	$\hat{U} = 1.1376$
S3 (rated)	$-0.2916 \pm j7.6980$	$\hat{U} = -0.2916$

For situations S1 and S3, it is easy to obtain their PCM models because however the wind speed varies under these two scenarios, the wind generator output will be kept constant. Thus the system structure will stay unchanged and so will the system critical eigenvalues. The corresponding results are shown in Table 5.

Until now, the system response in terms of an uncertain input has been modeled by means of PCM approximation. The obtained third order model is in a discontinuity form induced by the three different wind speed conditions.

### 5. Case study using a larger system

Now that its applicability has been verified in a simple system, the PCM-based uncertainty analysis will be conducted in this section for a larger system. A deeper understanding will be obtained by applying it to the SD voltage stability analysis.

#### 5.1. System description

A 6-machine 23-bus system to be examined has the single-line diagram shown in Fig. 5. This network contains six generator buses (Bus 1 to Bus 6), and six load buses (Bus 7 to Bus 12). The system raw data is originally provided by the commercial software PSS/E [26].

The SD voltage stability of this system is explored when the generator buses are replaced by the collector of wind generators one by one. The wind generator model used is the GE 3.6 MW DFIG-based WTG. The technical specifications of this model can be found in [27]. In the simulation, to replace the original Bus  $i$  generators with the capacity of  $P_i$ , a wind farm equipped with  $N(=P_i/3.6)$  DFIGs is assumed.

To make the application more realistic and representative, a Weibull distribution shown in Fig. 6 is applied to describe the wind speed probability distribution. (Note that if the proposed method is applied to an actual system, the local historical data should be used

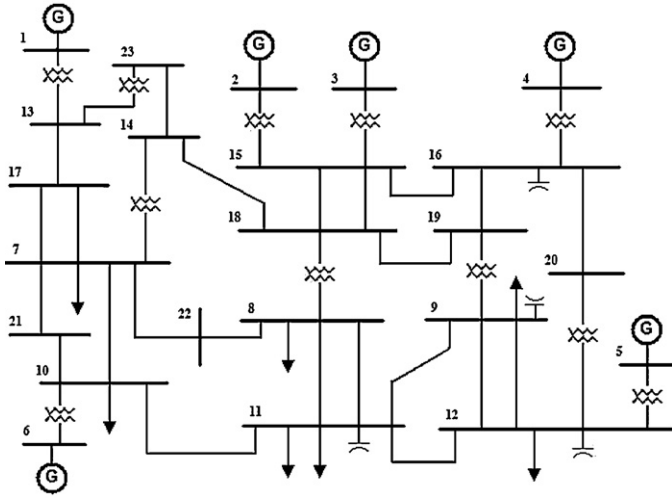


Fig. 5. Single-line diagram of the 6-machine 23-bus system.

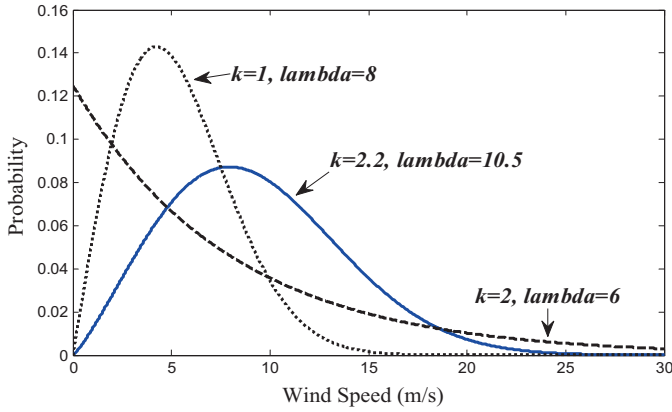


Fig. 6. Wind speed represented by Weibull distribution.

to specify the PDF of wind speed.) The PDF of a Weibull distribution is:

$$f(x; \lambda, k) = \begin{cases} \frac{k}{\lambda} \left(\frac{x}{\lambda}\right)^{k-1} e^{-(x/\lambda)^k}, & x \geq 0 \\ 0, & x < 0 \end{cases} \quad (21)$$

Weibull curves with different  $\lambda$  and  $k$  are shown in Fig. 6. The distribution with  $k=2.2$ ,  $\lambda=10.5$  is adopted.

## 5.2. PSDVS calculation

In [18,28], the system probabilistic small-signal stability is calculated as a stability index. Similarly, the system SD voltage stability could be evaluated in a probabilistic manner, and the probabilistic collocation method is an efficient tool to conduct this task.

In our research, the PCM is implemented to obtain the probability of small disturbance voltage stability (PSDVS). Computer programs are developed to calculate the PSDVS, which is illustrated in the flow chart of Fig. 7.

We will replace the Bus 1 generator with DFIG-based wind generators to demonstrate the calculation of PSDVS. First, the orthogonal polynomials need to be derived. For  $v_{wind}$  with Weibull distribution, the Associated Laguerre Polynomials [29] are deployed to derive the orthogonal polynomials. The derivation of orthogonal polynomials for Weibull distribution is detailed in Appendix B.

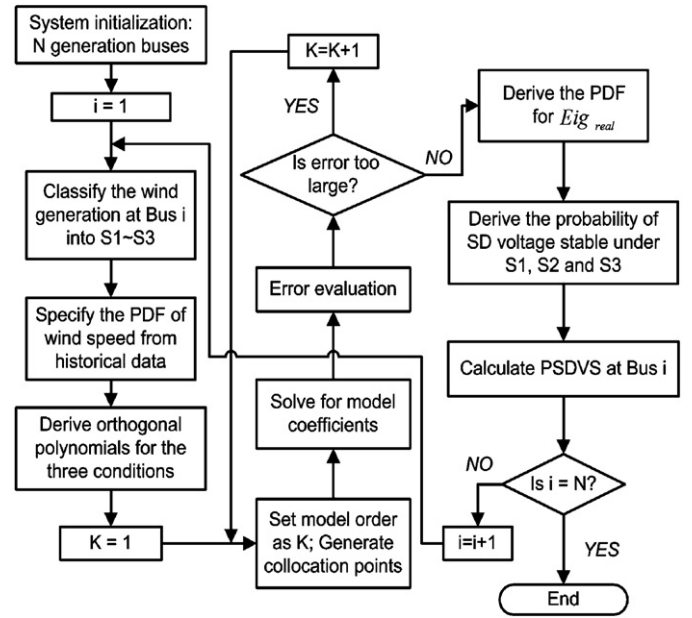


Fig. 7. Flow chart of the PSDVS calculation process.

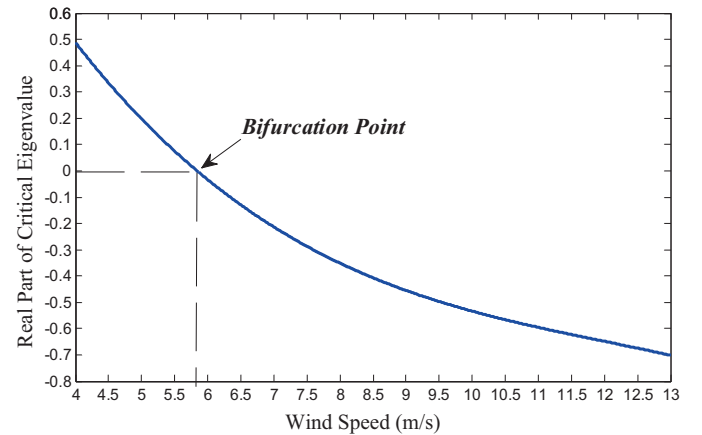


Fig. 8. Trajectory of  $Eig_{real}$  with the variation of  $v_{wind}$  under the situation of S2 using third-order PCM model.

The polynomial approximation for  $Eig_{real}$  is then obtained by means of the previously illustrated algorithm steps:  $Eig_{real} = \begin{cases} S1 : 0.4936 \\ S2 : C_0 = -0.454, C_1 = -0.179, C_2 = 0.051, C_3 = -0.011 \\ S3 : -0.7150 \end{cases}$

According to the above PCM model, the trajectory of  $Eig_{real}$  with the variation of  $v_{wind}$  under the situation of S2 is plotted in Fig. 8. From the discussion in Section 3, the voltage instability is possible depending whether or not the above eigenvalue passes the origin, which is also described in [4,5] as the dynamic bifurcation point.

It could be observed that  $Eig_{real}$  has been represented by a monotonic function of  $v_{wind}$  within S2. Given the PDF of random variable  $v_{wind}$  as  $f_X(v_{wind})$ , and the PCM monotonic model  $Eig_{real} = P_2(v_{wind})$ , the PDF of  $Eig_{real}$  could be calculated using the following equation [30]:

$$f_Y(y) = \left| \frac{1}{P_2'(P_2^{-1}(y))} \right| \times f_X(P_2^{-1}(y)) \quad (22)$$

where  $f_Y(y)$  is the PDF of  $Eig_{real}$ ,  $P_2^{-1}$  denotes the inverse function, and  $P_2'$  denotes the derivative. The meaning of this equation could be interpreted as follows: If the PDF of a random variable X is known

**Table 6**  
Comparative results using PCM and Monte Carlo method.

Bus No.	$E(\hat{Y})$	PSDVS			Dominant states
		PCM	MC 5000	MC 10,000	
1	-0.4544	87.5%	85.8%	87.9%	$E'_{q4}, \omega_5, \theta_5$
2	0.0347	42.3%	43.4%	42.6%	$E'_{q3}, \omega_3, \theta_3$
3	-0.0354	57.5%	56.2%	57.7%	$E'_{q2}, \theta_2, E'_{q5}$
4	-0.3219	81.6%	76.9%	80.1%	$E'_{q2}, E'_{q3}$
5	1.3822	0	0	0	$E'_{q2}, E'_{d3}$
6	0.0101	49.0%	47.8%	48.1%	$E'_{q4}$

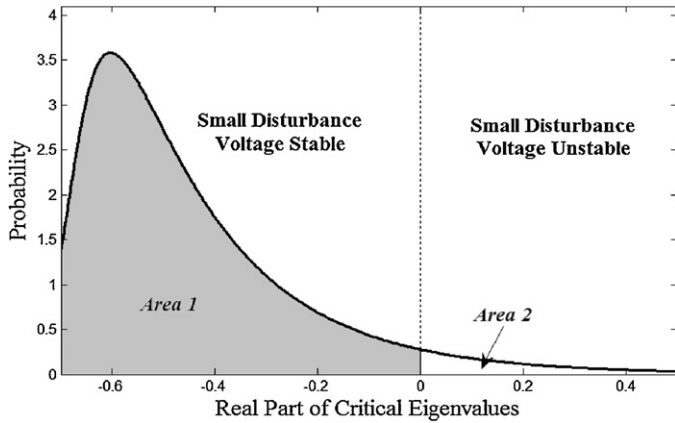


**Fig. 9.** PDF of  $Eig_{real}$  under the situation of S2 using third-order PCM model.

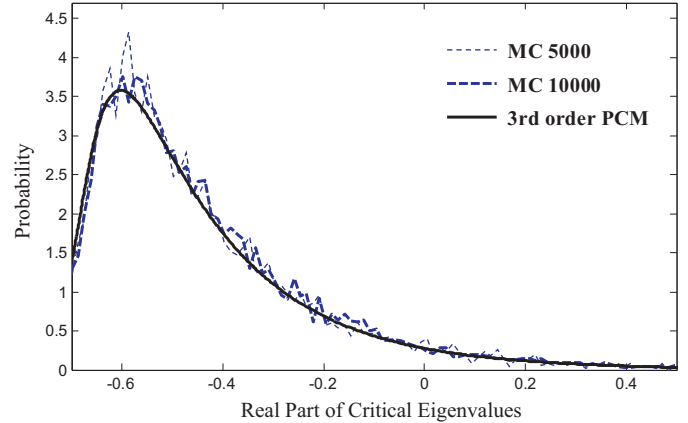


**Fig. 10.** Calculated probabilistic distribution of  $Eig_{real}$  under the situation of S2 using PCM and Monte Carlo method.

as  $f_X(x)$ , it is possible to calculate the PDF of some variable  $Y=g(X)$ . This is also called a “change of variable” and is in practice used to generate a random variable of arbitrary shape  $f_{g(X)}=f_Y$  using a known random number generator.

Implementing the above equation, the probability distribution of  $Eig_{real}$  is calculated and shown in Fig. 9.

Area 1 in Fig. 9 indicates the voltage is SD stable. The integral of Area 1 gives PSDVS under the situation of S2. From the analysis of previous section as well as simulation results, all  $Eig_{real}$  under S3 naturally falls on the stable side of the plane and all  $Eig_{real}$  under S1 are located on the unstable side. Two approaches could be used then to obtain the total PSDVS. One is the analytical method. Define  $f(U)$  as the probability of  $Eig_{real}$  at the value of  $U$ :

$$\begin{aligned}
 PSDVS &= \int_{S1}^{U<0} f(U)dU + \int_{S2}^{U<0} f(U)dU + \int_{S3}^{U<0} f(U)dU \\
 &= \left( \int_{S2}^{U<0} f(U)dU + \int_{S3}^{U<0} f(U)dU \right) \times 100\% \quad (23)
 \end{aligned}$$

The other approach approximates the PDF of  $Eig_{real}$  via a sufficient number of model simulations. Assuming that  $m$  out of  $n$  sample points are located on the stable side, then the PSDVS is represented as the ratio of  $m$  over  $n$ .

### 5.3. Numerical results

The PSDVS could be viewed as a voltage security index to reflect how the system would be SD stable if the traditional generators are replaced by wind generators at one particular bus. Table 6 gives the calculated PSDVS of each of the six generator buses in the 23-bus system. Meanwhile, using participation factors [6], the dominant state variables associated with each mode are obtained and listed in Table 6.  $E_d'$  and  $E_q'$  are the direct and quadrature axis components of the voltage behind the transient reactance,  $\delta$  is the rotor angular

displacement, and  $\omega$  is the rotor angular velocity. The subscript numbers stand for the most relevant generators in each mode.

The results shown in Table 6 provide useful information to be considered by the system designers while determining the optimum wind farm locations. Further, based on the calculation results, VAR arrangement strategy could be made for wind farm to adjust the reactive power output of DFIGs as well as the other reactive power compensators (SVC, STATCOM, etc.), and thus improve the voltage stability of the overall system.

Also listed in Table 6 are the numerical results obtained from traditional Monte Carlo method. This simulation-based approach is applied using 5000 samples and 10000 samples respectively. Simulation results are shown in Fig. 10 to compare with the results obtained by third order PCM model.

If the uncertainty analysis is conducted using the Monte Carlo approach from the beginning, thousands of simulations are needed to get the PDF of  $Eig_{real}$ . In comparison, with the ability to obtain the probabilistic distribution of  $Eig_{real}$  with similar accuracy, the third-order polynomial approximation method needs only four simulations for model derivation and a few more simulations for error evaluation. This could save a huge amount of time and computational resources. The PCM technique has exhibited great potential in the uncertainty analysis for wind generation.

## 6. Conclusions

In this paper, the issue of small disturbance voltage stability considering the nodal injection uncertainty of grid-connected DFIGs has been investigated and the following conclusions are reached:

- The probabilistic collocation method is introduced to perform the uncertainty analysis for wind generation. A classification of situations derived from the wind turbine cut-in, cut-out and rated wind speed is required. With the three situations specified, the PCM is applicable for small disturbance voltage stability analysis.

- Error evaluation is necessary for PCM to accurately represent the relationship between uncertain parameters and the outputs of interest. The PCM model with lower deviation from the real system enables a better approximation.
- The PCM is applied to a larger system. Simulation results indicate that the variation of wind farm output has considerable impact on the distribution of system critical eigenvalues. A deeper understanding could be obtained through the calculation of voltage security index PSDVS.
- As compared with the traditional simulation based approaches, the collocation method could provide quite an accurate approximation for the probabilistic distribution of system response with a much smaller number of model runs.

### Appendix A. Derivation of DFIG algebraic equations is provided below

Stator algebraic equations:

$$\begin{cases} V_{qs} = E'_q - R_s I_{qs} - X'_s I_{ds} \\ V_{ds} = E'_d - R_s I_{ds} - X'_s I_{qs} \\ P_s = V_{ds} I_{ds} + V_{qs} I_{qs} \\ Q_s = V_{qs} I_{ds} - V_{ds} I_{qs} \end{cases}$$

Rotor algebraic equations:

$$\begin{cases} V_{qr} = K_{p2}[K_{p1}(P_{ref} - P) + m_3 - I_{qr}] + m_4 \\ V_{dr} = K_{p4}[K_{p3}(Q_{ref} - Q) + m_1 - I_{dr}] + m_2 \\ P_r = V_{dr} I_{dr} + V_{qr} I_{qr} \\ Q_r = V_{qr} I_{dr} - V_{dr} I_{qr} \end{cases}$$

Other algebraic equations:

$$\begin{cases} I_{dr} = \frac{X_m}{X_r} I_{ds} + \frac{E'_q}{X_m} \\ I_{qr} = \frac{X_m}{X_r} I_{qs} - \frac{E'_q}{X_m} \\ P = P_r + P_s \\ Q = Q_r + Q_s \end{cases}$$

### Appendix B. Derivation of orthogonal polynomials for Weibull distribution

The Associated Laguerre Polynomials are orthogonal over  $[0, \infty)$  with respect to the measure with weighting function  $x^a e^{-x}$ :

$$\int_0^{\infty} x^a e^{-x} L_n^{(a)}(x) L_m^{(a)}(x) dx = 0 \quad (n \neq m)$$

Compare with the orthogonal polynomials with “Weibull” weighting function:

$$\int_0^{\infty} \left(\frac{x}{\lambda}\right)^{k-1} e^{-(x/\lambda)^k} H_n(x) H_m(x) dx = 0, \quad (n \neq m)$$

It can be seen that variable transformation needs to be performed. Similar to that of Gaussian distribution, we assume:

$$Y = \left(\frac{x}{\lambda}\right)^k$$

Substitute into the equation above, we have

$$\int_0^{\infty} Y^{(k-1)/k} e^{-Y} H_n(Y) H_m(Y) dY = 0, \quad (n \neq m)$$

Hence the associated Laguerre polynomials could be used considering the following:

$$\begin{cases} x = \lambda Y \bar{k} \\ a = \frac{k-1}{k} \end{cases}$$

The associated Laguerre polynomial of degree  $n$  is:

$$L_n^{(a)}(x) = \sum_{i=0}^n (-1)^i \binom{n+a}{n-i} \frac{x^i}{i!}$$

In our case:

$$a = \frac{k-1}{k} = 0.545$$

The first few orthogonal polynomials and collocation points are derived as follows:

$$\begin{aligned} H_0(Y) &= 1 \\ H_1(Y) &= -Y + 1.545 \\ H_2(Y) &= \frac{1}{2} Y^2 - 2.545Y + 1.966 \\ H_3(Y) &= -\frac{1}{6} Y^3 + 1.773Y^2 - 4.511Y + 2.323 \end{aligned}$$

Note that  $Y$  is an intermediate variable. Once the collocation points are determined, they will be transformed back to corresponding wind speeds. The 1st to 5th order collocation points and corresponding wind speeds are provided below:

Order	Collocation points	Corresponding wind speed (m/s)
1st	{1.5450}	{12.7958}
2nd	{0.9497, 4.1403}	{10.2566, 20.0290}
3rd	{0.6899, 2.8437, 7.1044}	{8.8697, 16.885, 25.6004}
4th	{0.5426, 2.1938, 5.1911, 10.2525}	{7.9524, 15.0065, 22.1977, 30.2453}
5th	{0.4474, 1.7913, 4.1501, 7.8057, 13.5305}	{7.2848, 13.6857, 20.0505, 26.7197, 34.3102}

### References

- [1] T. Van Cutsem, C. Vournas, Voltage Stability of Electric Power Systems, Kluwer Academic Publishers, Boston, 1998.
- [2] P. Kessel, H. Glavitsch, Estimating the voltage stability of a power system, IEEE Trans. Power Deliv. 1 (1986) 346–354.
- [3] M. Brucoli, F. Rossi, F. Torelli, M. Trovato, A generalized approach to the analysis of voltage stability in electric power systems, Electr. Power Syst. Res. 9 (1985) 49–62.
- [4] N. Yorino, H. Sasaki, Y. Masuda, et al., An investigation of voltage instability problems, IEEE Trans. Power Syst. 7 (1992) 600–611.
- [5] C.D. Vournas, P.W. Sauer, M.A. Pai, Relationships between voltage and angle stability of power systems, Electr. Power Energy Syst. 18 (1996) 493–500.
- [6] Prabha Kundur, Power System Stability and Control, McGraw-Hill, New York, 1994.
- [7] N. Amjady, M.R. Ansari, Small disturbance voltage stability evaluation of power systems, in: IEEE Transmission and Distribution Conference and Exposition, 2008.
- [8] W. Freitas, L.C.P. DaSilva, A. Morelato, Small-disturbance voltage stability of distribution systems with induction generators, IEEE Trans. Power Syst. 20 (2005) 1653–1654.
- [9] Z. Lubosny, Wind Turbine Operation in Electric Power Systems, Springer, New York, 2003.
- [10] B. Venkatesh, A. Rost, L. Chang, Dynamic voltage collapse index—wind generator application, IEEE Trans. Power Deliv. 22 (2007) 90–94.
- [11] F. Zhou, G. Joos, C. Abbey, Voltage stability in weak connection wind farms, Proceedings of IEEE PES General Meeting (2005).
- [12] N.R. Ullah, T. Thiringer, Variable speed wind turbines for power system stability enhancement, IEEE Trans. Energy Convers. 22 (2007) 52–60.
- [13] E. Muljadi, C.P. Butterfield, B. Parsons, A. Ellis, Effect of variable speed wind turbine generator on stability of a weak grid, IEEE Trans. Energy Convers. 22 (2007) 29–36.
- [14] C. Zheng, M. Kezunovic, Distribution system voltage stability analysis with wind farms integration, in: IEEE PES 42nd North America Power Symposium, Arlington, TX, USA, 2010.

- [15] V. Vittal, J. McCalley, V. Ajjarapu, U.V. Shanbhag, Impact of increased DFIG wind penetration on power systems and markets, PSERC Project Report, 2009–2010, available: [http://www.pserc.wisc.edu/research/public\\_reports/systems.aspx](http://www.pserc.wisc.edu/research/public_reports/systems.aspx).
- [16] F. Mei, B. Pal, Modal analysis of grid-connected doubly fed induction generators, *IEEE Trans. Energy Convers.* 22 (2007) 728–736.
- [17] H.A. Pulgar-Painemal, P.W. Sauer, Power system modal analysis considering doubly-fed induction generators, in: IREP Symposium on Bulk Power System Dynamics and Control, 2010.
- [18] C. Wang, L. Shi, L. Wang, Y. Ni, M. Bazargan, Modeling analysis in power system small signal stability considering uncertainty of wind generation, in: Proceedings of IEEE PES General Meeting, 2010.
- [19] M.A. Tatang, Direct Incorporation of Uncertainty in Chemical and Environmental Systems, Ph.D. dissertation, Massachusetts Institute of Technology, Cambridge, 1995.
- [20] M. Webster, M.A. Tatang, G.J. Mcrae, Application of the probabilistic collocation method for an uncertainty analysis of a simple ocean model, in: Joint Program on the Science and Policy of Global Change, MIT, Cambridge, MA, 1996, Tech. Rep. 4.
- [21] J.R. Hockenberry, B.C. Lesieutre, Evaluation of uncertainty in dynamic simulations of power system models: the probabilistic collocation method, *IEEE Trans. Power Syst.* 19 (2004) 1483–1491.
- [22] D. Han, J. Ma, R. He, Effect of uncertainties in parameters of load model on dynamic stability based on probabilistic collocation method, in: Proceedings of the IEEE 2007 Power Tech., 2007.
- [23] P.J. Davis, P. Rabinowitz, *Methods of Numerical Integration*, Academic, New York, 1975.
- [24] M. El-Kateb, S. Abdelkader, M.S. Kandil, Linear indicator for voltage collapse in power systems, *IEE Proc. Gener. Transm. Distrib.* 144 (1997) 139–146.
- [25] S. Abdelkader, B. Fox, Voltage stability assessment for systems with large power generation, *Int. J. Power Syst. Optim.* 2 (2010) 99–104.
- [26] PTI, PSS/E Application Guide, vol. 1 [M], PSS/E Brochure, 2002.
- [27] GE Energy, 3.6 MW Wind Turbine Technical Specifications.
- [28] Z. Xu, Z.Y. Dong, P. Zhang, Probabilistic small signal analysis using Monte Carlo simulation, in: Proceedings of IEEE PES General Meeting, 2005.
- [29] M. Abramowitz, I.A. Stegun, *Orthogonal Polynomials*. Ch. 22 in *Handbook of Mathematical Functions with Formulas, Graphs, and Mathematical Tables*, 9th printing, Dover, New York, 1972.
- [30] N.G. Ushakov, Density of a probability distribution. In *Hazewinkel, Michiel, Encyclopedia of Mathematics*, SpringerLink, 2001.